

RSC Advances



This is an *Accepted Manuscript*, which has been through the Royal Society of Chemistry peer review process and has been accepted for publication.

Accepted Manuscripts are published online shortly after acceptance, before technical editing, formatting and proof reading. Using this free service, authors can make their results available to the community, in citable form, before we publish the edited article. This *Accepted Manuscript* will be replaced by the edited, formatted and paginated article as soon as this is available.

You can find more information about *Accepted Manuscripts* in the [Information for Authors](#).

Please note that technical editing may introduce minor changes to the text and/or graphics, which may alter content. The journal's standard [Terms & Conditions](#) and the [Ethical guidelines](#) still apply. In no event shall the Royal Society of Chemistry be held responsible for any errors or omissions in this *Accepted Manuscript* or any consequences arising from the use of any information it contains.

Effect of “push-pull” sensitizers with modified conjugation bridges on the performance of p-type dye-sensitized solar cells

Fengying Zhang, Pei Yu, Wei Shen, Ming Li, Rongxing He*

Key Laboratory of Luminescence and Real-Time Analytical chemistry (Southwest University), Ministry of Education, College of Chemistry and Chemical Engineering, Southwest University, Chongqing 400715, China

* To whom correspondence should be addressed. E-mail: herx@swu.edu.cn.

Abstract: A series of “push-pull” sensitizers with modified conjugation bridges are designed and investigated by density functional theory (DFT) and time-dependent density functional theory (TD-DFT), with the purpose of revealing the effect of different linker moieties on the performance of p-type dye-sensitized solar cells (DSSCs). Creatively, the electron-rich unit (thiophene) and the electron-deficient unit (pyrimidine) are explored as the linking groups in p-type sensitizers from a comparative perspective, two special bridge-sites and the lengths of conjugation bridges are also taken into account. Calculations of the highest occupied molecular orbital (HOMO) and the lowest unoccupied molecular orbital (LUMO) indicate that there are efficient hole injection and dye regeneration for all the sensitizers. Importantly, the influence of the number of thiophene and pyrimidine reflects mainly on the long-wavelength region and the short-wavelength region, respectively. Besides, according to the charge transfer properties and the driving forces of hole injection, dye regeneration and charge recombination (ΔG_{inj} , ΔG_{reg} and ΔG_{CR}), the increased length in thiophene-based bridge nearing the carboxyl has a positive impact on the device performance. Likewise, for the pyrimidine-based bridges, it is probably the increased conjugation length between the donor and acceptor could significantly improve the device efficiency. Our intensive analysis on the π -bridges provides assistance for designing more efficient p-type photosensitizers, which contributes to the rational design for tandem DSSCs.

Keywords: “push-pull” sensitizers, thiophene, pyrimidine, device performance

1. Introduction

Plenty of interests have been paid to dye-sensitized solar cells (DSSCs), the environment-friendly, low-cost and easy-preparation photoelectrochemical devices compared with traditional photovoltaic, since Grätzel and co-workers presented it in their seminal paper in 1991¹. To date, extensive researches on classical DSSCs (n-type DSSCs) vary from preparing new semiconductor^{2,3}, designing and synthesizing new dyes^{4,5} to exploring new electrolytic mass⁶ for the sake of perfecting optical performance of device and the power conversion efficiency (PCE) of battery effectively. Nevertheless, there is scarce exploration about the counterparts of n-type DSSCs, even though they play irreplaceable roles in inexpensive tandem devices (pn-type DSSCs)⁷⁻¹⁰. Theoretically, the tandem DSSCs can overcome the Shockley-Queisser limit efficiently by absorbing both high energy photons and lower energy photons at the corresponding bandgap junction, therefore, this tandem arrangement can be perceived as a kind of executable strategy to enhance the overall efficiency. Moreover, they possess greater potential with efficiency up to 43% when compared with the simplex n-type DSSCs whose theoretical efficiency is 30%. Actually, the highest PCE in record for tandem DSSCs is 2.42%¹¹, far below 13% which is realized in n-type DSSCs cosensitized by zinc-porphyrin in cobalt-based electrolyte¹². One of the major obstacles in pn-type DSSCs with poor photovoltaic performance is the mismatch of photocurrent between photoanode and photocathode. Thus, it is worth exploring and promoting p-type DSSCs with improved current densities.

Since the first self-operating p-type DSSCs was carried out on the erythrosine by Lindquist and coworkers¹³, plenty of potential sensitizers, including perylene, coumarin, porphyrin and their derivatives, have been explored in succession¹⁴⁻¹⁶. Until the discovery of a new-type sensitizer with the “push-pull” configuration: 4-(Bis-{4-[5-(2,2-dicyano-vinyl)-thiophene-2-yl]-phenyl-amino)-benzoic acid (P1), the PCE can reach 0.15% which is significantly higher than previous¹⁷⁻¹⁹. At current stage, with the application of abundant modification measures for improvement, the photocathode efficiency of 1.3% was gained by Spiccia and co-workers in p-type DSSCs²⁰.

Differing from the electron photoinjection into the conduction band of anode semiconductor such as TiO₂ in n-type DSSCs, the hole is injected into the inorganic semiconductor (NiO) from excited sensitizers followed by the electron transfer to the redox couple in electrolyte for p-type DSSCs^{8, 21-23}. Plenty of studies have shown that the rapid back speed of photoinjected hole from p-type semiconductor to reduced dye cuts down the separation efficiency of charges, so as to limit the incident photon-to-current conversion efficiencies (IPCEs) and resultant photocurrent^{24, 25}. One of the effective methods to improve the efficiency of charge separation is to increase the distance of charge transfer by employing longer bridge groups between the electron-withdrawing group (acceptor) and anchoring group when anchoring group attaches to the electron-donating group (donor)²⁶. Based on the typical “push-pull” sensitizer P1, Wu and coworkers²⁷ shed light on the effect of different π -bridges, indicating that 3,4-ethylenedioxythiophene was superior compared to thienyl and

phenyl in IPCE. Li and co-workers^{26, 28} synthesized and discussed the homologous sensitizer T1, in which an additional thiophene unit was inserted between the triphenylamine and carboxylic groups. They concluded that the performance of the device was improved significantly when the length of bridge ligand nearing the anchoring group increases, while, the increased conjugation bridge between the donor and acceptor had a negative effect on the device efficiency.

To further comprehend and demonstrate the effect of conjugation bridges of “push-pull” dyes on the device performance, a series of p-type sensitizers with modified conjugation bridges are designed and calculated. Herein, our primary interest in two kinds of bridges, one nears the anchoring group (D-bridge) and another lies between the donor and acceptor (A-bridge), is to explore their difference for battery performance by employing electronic-deficient pyrimidin and electron-rich thiophene, respectively. What’s more, the influences of their lengths are also taken into consideration. We believe that the better understanding of π -bridges, including their different induced effects of electron, positions and lengths, could provide guidance for the further study of p-type sensitizers with higher PCE.

2. Methods

2.1 Theoretical background

To the best of our knowledge, as the benchmark of solar cell performance for p-type DSSCs, the energy conversion efficiency (η) is closely correlated with three factors: short-circuit photocurrent density (J_{sc}), open-circuit photovoltage (V_{oc}) and

fill factor (FF), as follows²⁹:

$$\eta = \frac{J_{sc} V_{oc}}{I_s} FF \quad (1)$$

Where, I_s represents the total solar power incident on the cell.

As one of the important parameters in the theoretical study for DSSCs, J_{sc} can be evaluated by the following integral equation^{7, 30, 31}:

$$J_{sc} = e \int_{\lambda} LHE(\lambda) \Phi_{inj} \eta_{reg} \eta_{coll} I_s(\lambda) d\lambda \quad (2)$$

Where, $LHE(\lambda)$ represents the light-harvesting efficiency at a concrete wavelength, Φ_{inj} is the electron injection efficiency, η_{reg} and η_{coll} denote the regeneration efficiency of the oxidized dye and the charge collection efficiency, respectively. In equation (2), $LHE(\lambda)$ is determined by the oscillator strength (f) of the absorbed dye molecule at maximum wavelength λ_{max} . Φ_{inj} is associated with the driving force of hole injection (ΔG_{inj}) from the excited dye to the semiconductor. Furthermore, η_{reg} can be also measured by the driving force of regeneration (ΔG_{reg}) between the oxidized dye and electrolyte. They are listed via the following expression^{8, 32}:

$$LHE = 1 - 10^{-f} \quad (3)$$

$$\Delta G_{inj} = e [E_{VB}(\text{NiO}) - (E_{0-0} + E_{red}(\text{Dye}))] \quad (4)$$

$$\Delta G_{reg} = e [E(I_2/I_3^-) - E_{red}(\text{Dye})] \quad (5)$$

As for V_{oc} , the other determinant factor for evaluating the performance of DSSCs, it can be expressed as follows⁸:

$$V_{oc} = E(I^-/I_3^-) - E_F(\text{NiO}) \quad (6)$$

Where, $E(I^-/I_3^-)$ and $E_F(\text{NiO})$ are the Fermi levels of electrolyte iodine/iodide (I^-/I_3^-) and semiconductor NiO. Notably, $E_F(\text{NiO})$ is closely linked to the hole injection and

charge recombination processes in DSSCs.

Additionally, the process of unfavorable charge recombination can be evaluated by its corresponding free energies ΔG_{CR} , which can be expressed as^{8,32}:

$$\Delta G_{CR} = e[E_{red}(\text{Dye}) - E_{VB}(\text{NiO})] \quad (7)$$

Where, $E_{red}(\text{Dye})$ is the reduction potential of dye, $E_{VB}(\text{NiO})$ represents the energy of the valence band of NiO.

For the reorganization energy of S1 excited state $E_{reorg}(S1)$, it is determined by the difference of $E_{S1}(Q0)$ and $E_{S1}(Q1)$,^{33,34}:

$$E_{reorg}(S1) = E_{S1}(Q0) - E_{S1}(Q1) \quad (8)$$

Where, $E_{S1}(Q0)$ and $E_{S1}(Q1)$ represent the energies of S1 states corresponding to equilibrium geometries Q0 and Q1, respectively. Based on the equation (8), E_{0-0} can be gained as follows^{33,34}:

$$E_{0-0} = E_{\lambda_{max}} - E_{reorg}(S1) \quad (9)$$

Where, $E_{\lambda_{max}}$ represents the energy of the maximum absorption.

2.2 Computational details

Geometry optimizations of all the objected dye molecules in their ground states are performed on the basis of density functional theory (DFT). Several functionals (M062X, LC-WB97XD, PBE0, B3LYP) are applied for obtaining the appropriate energy levels consisted with experiments (results shown in **Table S1**), it can be easily found that PBE0/6-31G(d) is enough for the present system. Thus, in the whole research, for all the isolated sensitizers (Dyes) and their complexes linked with semiconductor (NiO/Dyes), the hybrid functional PBE0 combined with the 6-31G(d)

basis set is employed for C, H, O, N, S atoms, simultaneously, the double- ξ (DZ) basis set LanL2DZ with corresponding pseudopotential is employed for Ni atom. Taking the nickel oxide clusters into account, clusters NiO and (NiO)₉ are gained in Materials Studio 7.0, and their structures are optimized at DFT/PBE0/LanL2DZ level. Moreover, on the basis of the optimized ground-state geometries, the excited states of all the sensitizers are calculated with time-dependent density functional theory (TD-DFT), Boese and Martin's τ -dependent hybrid functional (BMK) together with 6-31G(d) is used for their vertical electronic excitation energies and spectra simulation (calculations by other different functionals are listed in **Table S2**). Additionally, the polarized continuum model (PCM) is adopted throughout, and acetonitrile is taken as the solvent in the whole investigation for evaluating solvent effects based on the experimental settings. What's more, frequency calculations are used for all the geometry optimizations with the purpose of implying no imaginary. All the relevant calculations are carried out in the Gaussian 09 program package³⁵.

To measure the nature of photoinduced electron-hole separation in depth, related electron densities of sensitizers are calculated by code Multwfn 2.5³⁶. Correspondingly, the distance of charge transfer and the fraction of charge exchange are calculated with *DctViaCube*³⁷.

3. Results and discussion

3.1 Molecular geometries and electronic properties

It is well known that π -bridges of dyes with "push-pull" structures have great

influence on the light absorption, separation of the electron-hole pairs, charge transfer properties and so on³⁸⁻⁴². For the purpose of investigating the influence of linker moiety on the IPCEs and structure-property relationships in p-type DSSCs, several sensitizers, employing two kinds of typical groups (pyrimidine units and thiophene units) with different induced effects of electron as π -linkers, are calculated and studied based on the 5-(4-(bis(4-(5-(2,2-dicyano-vinyl)-thiophen-2-yl)phenyl)amino)-phenyl)thiophene-2-carboxylic acid (T1, also called T-D-1S-A-1S). Other molecules are named by the form of T-D-xX-A-yY, where X is N or S, Y is N or S. D and A represent the donor part and acceptor part, respectively. N and S denote pyrimidine and thiophene, respectively. x is 1, 2 or 3, y is 1, 2 or 3), their specific names and structures are presented in **Fig. 1**. Results of optimized geometries indicate that there are some certain discrepancies for electron-deficient groups (pyrimidine units) and electron-rich groups (thiophene units) in terms of the dihedral angle between the donor (triphenylamine, TPA) and π -bridge. Corresponding with previous researches, the dihedral angles between the phenyl in TPA and thiophene are approximately 21° when thiophene groups are taken as the linker moieties³¹, which are ascribed to their slight steric hindrance of H atoms. However, as for sensitizers with pyrimidine-based bridges, there are almost no reverse between pyrimidine and TPA. It is worth noting that conjugation degree and physical properties are pertinent to the π -linker fragment. The difference in conjugation degree for thiophene units and pyrimidine units implies that pyrimidine-based dyes possess better ability of electron delocalization due to the good planarity, however, the unfavorable conjugation of thiophene-based dyes may

induce the localization of frontier molecular orbitals (FMOs), leading to the efficient separation of hole-electron pairs, reducing their combination advantageously³¹. In addition, different positions and lengths of π -bridges in dyes show little impact on structures' reverse.

Generally, the electronic excitation of dyes as well as their transition characters are closely correlated with their FMOs^{43, 44}: the highest occupied molecular orbital (HOMO) and the lowest unoccupied molecular orbital (LUMO). As presented in **Fig. 2**, all the dyes show high LUMO energy levels for efficient electron transfer to the electrolyte ($E(I_2/I_3^-) = -4.15 \text{ eV}^{26}$), the sufficiently low HOMO energy levels for efficient hole injection into the semiconductor NiO ($E(\text{NiO}) = -5.04 \text{ eV}^{26}$). Depending on the change of bridges in length, calculations suggest that energies of HOMO and LUMO become higher slightly with the lengths of bridges increasing. On the one hand, thiophene-based bridges impact mainly on the HOMO energy level, and pyrimidine-based bridges nearing the acceptor have great influences on both HOMO and LUMO energy levels. However, on the other hand, energies of HOMO and LUMO are almost unchanged when D-bridge is pyrimidine unit. Moreover, it can be speculated from the different energies between HOMO and LUMO that the decreased band gaps realized in longer bridges are conducive to the red shift of spectra.

To the best of our knowledge, for the ideal sensitizers which have fast hole injection from the excited state of dye into the valence band of NiO, the HOMOs of dyes should be predominantly delocalized over the anchoring groups and their surroundings, the LUMOs distributions of dyes should extend on the acceptor groups

and keep away from semiconductor with the purpose of reducing hole recombination²⁶. All the distributions of HOMOs in our research systems are significantly located on the donor groups and their adjacent bridge-rings. As for the LUMOs, they are distributed mainly on the acceptor groups and their surroundings. Notably, with the lengthening of π -bridges, the distributions of LUMOs are increasingly far away from TPA, which is probably beneficial to the superior hole injection.

3.2 Optical properties

The absorption spectra of sensitizers are the powerful parameters repeatedly employed to evaluate their abilities of light-harvesting. To investigate the optical properties of dyes in our research system, the electronic spectra of isolated sensitizers and sensitizers linked with nickel oxide in acetonitrile are simulated and presented in **Fig. 3**. Apparently, two kinds of major absorption bands appearing in the short wavelength region (300-450 nm) and long wavelength region (500-650 nm) region are gained in the absorption spectrogram, which are assigned to the B band and Q band, respectively^{34, 45, 46}. Interrelated electronic transition data about the main absorption peaks in B band and Q band are collected in **Table S3**.

It is noted from **Fig. 3** that absorption spectra of all the dyes are affected scarcely no matter whether sensitizers linked with the semiconductor NiO. For two systems, sensitizers linked with nickel oxide (NiO-Dyes and (NiO)₉-Dyes, their optimized structures are presented in **Fig. S1**), both of them can simulated spectral features commendably, their calculated spectra agree better with that of isolated dyes. Based

on the further analysis of spectra, the maximum wavelength of spectral absorption in Q band appears red-shift obviously with the lengths of thiophene-based bridges directly linked with acceptor groups increasing, from 498 nm (T-D-1S-A-1S), 527 nm (T-D-1S-A-2S) to 543 nm (T-D-1S-A-3S). In addition, the absorption strength also has a great improvement, the maximal oscillator strength of 3.3 is gained in T-D-1S-A-3S (from **Table 1**). For pyrimidine-based bridges closing acceptor groups, they have a significant influence on the B band. The absorption at 300–400 nm is enhanced dramatically as the lengths of pyrimidine-based A-bridges increase. In the case of D-bridges, regardless of thiophene units or pyrimidine units, they have little effect on the absorption spectra. With respect to the different π -bridges (thiophene-based bridges and pyrimidine-based bridges), the comparison of their absorption spectra implies that dye molecules with thiophene units as the conjugation bridges have better ability to capture the light.

To clarify the light absorption properties of dyes visually and accurately, some key parameters are gathered in **Table 1**. It is well known that f reflects light-harvesting efficiency (LHE) to a certain extent owing to the limited dye loading on the semiconductor film¹⁸. As expressed in equation (3), the stronger the f , the larger the LHE . According to the analysis of the Q band, the largest LHE of 0.9995 achieved in T-D-1S-A-3S is not prominent in comparison to the 0.9859 of T-D-1S-A-1S. In contrast, the difference value of 0.35 in f leads to the change of LHE from 0.9859 (T-D-1S-A-1S) to 0.9499 (T-D-1S-A-3N). Summarily, LHE has no significant change for dyes in the Q band. With respect to the B band, the increase of oscillator strength

to 1.62 is realized in T-D-1S-A-2N in comparison with 0.73 (T-D-1S-A-1S). Correspondingly, its *LHE* is improved to 0.976 compared with 0.8138 (T-D-1S-A-1S), which is conducive to the capture of sunlight in the short wavelength region.

As for the transition dipole moment from states S0 to S1 (μ_T), it is another way to confirm the ability of light-harvest and electron-transition. As shown in **Table 1**, μ_T is enhanced in the order of T-D-1S-A-1S (30.28) < T-D-1S-A-2S (33.03) < T-D-1S-A-3S (58.97), T-D-1N-A-1S (29.99) < T-D-2N-A-1S (30.03) < T-D-3N-A-1S (30.07). These sequences manifest that μ_T is dramatically increased with thiophene-based A-bridge lengthening, but for pyrimidine-based D-bridges, μ_T has a little change. Inversely, it is decreased as T-D-1S-A-1S (30.28) > T-D-2S-A-1S (29.34) > T-D-3S-A-1S (28.70), T-D-1S-A-1N (26.41) > T-D-1S-A-2N (24.26) > T-D-1S-A-3N (20.70), these orders reveal the conclusion that the longer the thiophene-based D-bridges, as well as pyrimidine-based A-bridges, the smaller the μ_T .

Considering the reorganization energy of S1 excited state $E_{\text{reorg}}(\text{S1})$, it increases with the lengthening of A-bridge, exactly as T-D-1S-A-1S (0.13) < T-D-1S-A-2S (0.15) < T-D-1S-A-3S (0.18), T-D-1S-A-1N (0.07) < T-D-1S-A-2N (0.08) < T-D-1S-A-3N (0.10). But for the change of thiophene-based D-bridges, the smaller $E_{\text{reorg}}(\text{S1})$ realized in T-D-3S-A-1S (0.10). The identical $E_{\text{reorg}}(\text{S1})$ (0.14) appears in the sensitizers with pyrimidine units as bridges.

3.3 Charge transfer properties

In general, for the “push-pull” dyes whose anchoring groups located on the electron donor parts in p-type DSSCs, the electrons are transferred from the semiconductors to

the donor parts of sensitizers following the hole-injection through the conjugated D-bridges. In order to investigate some details of the charge transfer properties, including the electron transfer distance (L in Å), the fraction of electron exchange ($\Delta\epsilon$ in $|e^-|$), as well as the overlaps between the areas of density depletion and increment (Ω , Isovalue: $4 \times 10^{-4} e \text{ au}^{-3}$), electron density difference plots of electronic transition $S_0 \rightarrow S_1$ for all the isolated dyes and dyes linked with nickel oxide (NiO-Dyes and (NiO)₉-Dyes) are calculated and listed in **Table 2** and **Table S4**, respectively.

From **Table 2**, the electron density depletion (green) localizes largely on the anchoring groups, conjugation spacers and donor parts, nevertheless, the electron density increment (purple) mainly localizes on the acceptor segments, which contributes to the electron moving from the green area to the purple area. Besides, the zones of overlaps for the electron density depletion and increment occur in the A-bridges and their surroundings. Interestingly, the length of the electron transfer reflects the overlaps between the regions of density depletion and increment roughly in some degree. The longer the charge transfer distance, the less overlaps for the electron density, accordingly, it leads to a good charge separation. For the situation of (a) in **Table 2**, when the conjugation moieties in the A-bridges are two thiophenes, the Ω is only 0.1934, corresponding L reaches a length of 6.219. However, when the number of thiophene is up to 3, the electron transfer distance reduces to 3.780, and the Ω becomes 0.3601. The results indicate that the longer the thiophene-based bridges between the donor and acceptor do not correspond to the better charge separation, it is probably the nonlinear change of charge distributions as the number of thiophene

increases, the increased thiophene units in A-bridges do not promote the charge separation^{47, 48}. For (c), the good charge separation is realized in different pyrimidine-based A-bridges, complying with the sequence of T-D-1S-A-1N (L= 4.515, $\Delta e = 1.1681$, $\Omega = 0.2726$) < T-D-1S-A-2N (L= 6.261, $\Delta e = 1.2914$, $\Omega = 0.1264$) < T-D-1S-A-3N (L= 8.023, $\Delta e = 1.3276$, $\Omega = 0.0522$). The tendency implies that charge separation is enhanced significantly by lengthening pyrimidine units in the A-bridges. Furthermore, changes on the D-bridges suggest that the electron transfer distance and the fraction of electron exchange can be improved dramatically for the thiophene-based bridges, but almost are equal for the pyrimidine-based bridges.

What's more, for NiO-Dyes and (NiO)₉-Dyes presented in **Table S4**, it can be obtained obviously that there are similar character of the charge transfer between dyes linked with nickel oxide and isolated dyes. In the (NiO)₉-Dyes, three molecules, ((NiO)₉-T-D-1S-A-1S, (NiO)₉-T-D-2S-A-1S and (NiO)₉-T-D-2N-A-1S), extend a special way of electron transfer. The electron density depletion of them localizes partly on nickel oxide, which indicates that their electron densities move from (NiO)₉ to the acceptor area.

3.4 Important performance parameters

Based on the equations discussed in the theoretical background, it is observed that sensitizers play an important role in *LHE*, Φ_{inj} and η_{reg} during the photoelectric conversion process, so as to exert great influence on the η through J_{sc} and V_{oc} .

The *LHE* has been evaluated by f in the section of optical properties. It is well established that absorption spectra in Q band are affected primarily by the

electron-rich thiophene units, especially when they are located in the A-bridges. Conversely, the electronic-deficient pyrimidine groups exert a great influence on the absorption spectra in the B band, particularly when it is taken as the A-bridges. In addition, redox potentials of all the dyes are also calculated and analyzed, results are collected in **Table 3**. The electron injection driving force ΔG_{inj} , a key parameter associated with electron injection efficiency Φ_{inj} , is calculated on the basis of equation (4). It is easy to be found that ΔG_{inj} is minished a little with the lengths of thiophene-based A-bridges increasing. For the other situation, when the number of thiophene and pyrimidine nearing the COOH increases, the change of ΔG_{inj} is negligible. To be pleasant, the $-\Delta G_{inj}$ is increased in the order of 0.76 (T-D-1S-A-1N) < 0.88 (T-D-1S-A-2N) < 0.98 (T-D-1S-A-3N) for the increment of pyrimidine-based A-bridges. Subsequently, the key regeneration process in DSSCs device has also been evaluated roughly through ΔG_{reg} , according to the equation (5). Correlated data of ΔG_{reg} in **Table 3** elucidate that sensitizers (T-D-2S-A-1S and T-D-3S-A-1S) possess the greatest driving force of regeneration 0.94 eV compared with other dyes. Actually, previous literatures^{49, 50} have revealed that both electron injection and dye regeneration can be occurred efficiently when the driving force is larger than 0.2 eV. As a whole, all the sensitizers have effective injection and regeneration.

Besides these, based on the equation (7), the process of unfavorable charge recombination is also discussed and analyzed. From **Table 3**, it is not difficult to find that all the ΔG_{CR} for dyes are positive, which are in favor of hindering the charge recombination. For T-D-1S-A-1S, the great ΔG_{CR} of 1.82 is gained, and with the

number of thiophene in D-bridge increasing, the ΔG_{CR} of 1.83 appears in T-D-2S-A-1S and T-D-3S-A-1S. With respect to the increase of lengths for A-bridges, including thiophene-based bridges and pyrimidine-based bridges, the ΔG_{CR} complies with the sequences of 1.82 (T-D-1S-A-1S) > 1.75 (T-D-1S-A-2S) > 1.71 (T-D-1S-A-3S), 1.66 (T-D-1S-A-1N) > 1.53 (T-D-1S-A-2N) > 1.49 (T-D-1S-A-3N). Summarily, inserting thiophene groups as the D-bridge can well modify the sensitizers' energy levels and lead to the lower charge recombination. Actually, according to the above analysis of important performance parameters, corresponding tendencies are presented intuitively in **Fig. S2**.

4. Conclusions

In conclusion, modified conjugation bridges of “push-pull” sensitizers play a vital role in the performance of p-type DSSCs. Two types of groups (thiophene and pyrimidine) with different induced effects of electron are discussed comparatively throughout, in addition, the locations of bridges (A-bridge and D-bridge) as well as their lengths are also included in the calculation. Based on the geometries, dyes containing pyrimidine-based bridges exhibit greater planarity than dyes with thiophene-based bridges. It is valuable to note that all the designed sensitizers possess sufficient energies for hole injection and dye regeneration due to the lower HOMO than the VB of NiO and the higher LUMO than the redox potential of I_2/I_3^- . Moreover, related exploration on optical properties implies that there is a significant influence on the Q band with the lengths of thiophene-based D-bridges increasing. In contrast,

increased lengths for pyrimidine-based A-bridges can lead to the strengthening of spectra in B band. As for the analysis of the charge transfer properties, sensitizers with thiophene units as the D-bridges and pyrimidine units as the A-bridges exert the longer charge transfer distances and more electron exchange as the lengths of bridges increase.

Fundamentally and practically, these critical parameters (ΔG_{inj} , ΔG_{reg} and ΔG_{CR}) are closely associated with the performance of p-type DSSCs, particularly for the J_{sc} and charge recombination. Related analysis indicates that increased lengths of thiophene units in the D-bridges have little influence on ΔG_{inj} , ΔG_{reg} and ΔG_{CR} , but for the pyrimidine units in the A-bridges, they exhibit favorable influence on the charge injection and recombination. Combined with previous researches, we confirmed again that the increased lengths in thiophene-based bridges near the carboxyl have a positive effect on the device performance. Similarly, for the pyrimidine-based bridges, it can be speculated that the increased conjugation lengths in the A-bridges could significantly improve the device efficiency. In addition, compared thiophene units with pyrimidine units, it probably that pyrimidine units have better contribution to the device efficiency relatively in our designed sensitizers. These results provide much guidance for the future design of p-type “push-pull” sensitizers with higher PCE.

Acknowledgement

We acknowledge the generous financial support from Natural Science Foundation of China (21173169), Chongqing Municipal Natural Science Foundation

(cstc2013jcyjA90015), and the Fundamental Research Funds for the Central Universities (No. XDJK2013A008).

References

1. B. O'regan and M. Grätzel, *nature*, 1991, 353, 737-740.
2. Z. Yang, T. Xu, S. Gao, U. Welp and W.-K. Kwok, *The Journal of Physical Chemistry C*, 2010, 114, 19151-19156.
3. B. Lei, J. Liao, R. Zhang, J. Wang, C. Su and D. Kuang, *The Journal of Physical Chemistry C*, 2010, 114, 15228-15233.
4. H. Imahori, T. Umeyama and S. Ito, *Accounts of Chemical Research*, 2009, 42, 1809-1818.
5. D. Kuang, S. Ito, B. Wenger, C. Klein, J.-E. Moser, R. Humphry-Baker, S. M. Zakeeruddin and M. Grätzel, *Journal of the American Chemical Society*, 2006, 128, 4146-4154.
6. J. Shi, B. Peng, J. Pei, S. Peng and J. Chen, *Journal of Power Sources*, 2009, 193, 878-884.
7. F. Odobel, Y. Pellegrin, E. A. Gibson, A. Hagfeldt, A. L. Smeigh and L. Hammarström, *Coordination chemistry reviews*, 2012, 256, 2414-2423.
8. F. Odobel, L. c. Le Pleux, Y. Pellegrin and E. Blart, *Accounts of chemical research*, 2010, 43, 1063-1071.
9. F. Odobel and Y. Pellegrin, *The Journal of Physical Chemistry Letters*, 2013, 4, 2551-2564.
10. A. Baranwal, T. Shiki, Y. Ogomi, S. Pandey, T. Ma and S. Hayase, *RSC Advances*, 2014, 4, 47735-47742.
11. A. Nattestad, A. J. Mozer, M. K. Fischer, Y.-B. Cheng, A. Mishra, P. Bäuerle and U. Bach, *Nature materials*, 2010, 9, 31-35.
12. S. Mathew, A. Yella, P. Gao, R. Humphry-Baker, B. F. Curchod, N. Ashari-Astani, I. Tavernelli, U. Rothlisberger, M. K. Nazeeruddin and M. Grätzel, *Nature chemistry*, 2014, 6, 242-247.
13. J. He, H. Lindström, A. Hagfeldt and S.-E. Lindquist, *The Journal of Physical Chemistry B*, 1999, 103, 8940-8943.
14. A. Morandeira, J. Fortage, T. Edvinsson, L. Le Pleux, E. Blart, G. Boschloo, A. Hagfeldt, L. Hammarström and F. Odobel, *The Journal of Physical Chemistry C*, 2008, 112, 1721-1728.
15. A. Morandeira, G. Boschloo, A. Hagfeldt and L. Hammarstrom, *The Journal of Physical Chemistry C*, 2008, 112, 9530-9537.
16. H. Zhu, A. Hagfeldt and G. Boschloo, *The Journal of Physical Chemistry C*, 2007, 111, 17455-17458.
17. P. Qin, H. Zhu, T. Edvinsson, G. Boschloo, A. Hagfeldt and L. Sun, *Journal of the American Chemical Society*, 2008, 130, 8570-8571.
18. L. Li, E. A. Gibson, P. Qin, G. Boschloo, M. Gorlov, A. Hagfeldt and L. Sun, *Advanced Materials*, 2010, 22, 1759-1762.
19. Y.-S. Yen, W.-T. Chen, C.-Y. Hsu, H.-H. Chou, J. T. Lin and M.-C. P. Yeh, *Organic letters*, 2011, 13, 4930-4933.
20. S. Powar, T. Daeneke, M. T. Ma, D. Fu, N. W. Duffy, G. Götz, M. Weidelener, A. Mishra, P.

- Bäuerle and L. Spiccia, *Angewandte Chemie*, 2013, 125, 630-633.
21. M. Borgström, E. Blart, G. Boschloo, E. Mukhtar, A. Hagfeldt, L. Hammarström and F. Odobel, *The Journal of Physical Chemistry B*, 2005, 109, 22928-22934.
 22. A. Morandeira, G. Boschloo, A. Hagfeldt and L. Hammarström, *The Journal of Physical Chemistry B*, 2005, 109, 19403-19410.
 23. J. Preat, A. Hagfeldt and E. A. Perpète, *Energy & Environmental Science*, 2011, 4, 4537-4549.
 24. F. Vera, R. Schrebler, E. Munoz, C. Suarez, P. Cury, H. Gómez, R. Córdova, R. Marotti and E. Dalchiele, *Thin Solid Films*, 2005, 490, 182-188.
 25. S. Mori, S. Fukuda, S. Sumikura, Y. Takeda, Y. Tamaki, E. Suzuki and T. Abe, *The Journal of Physical Chemistry C*, 2008, 112, 16134-16139.
 26. L. Zhu, H. Yang, C. Zhong and C. M. Li, *Chemistry-An Asian Journal*, 2012, 7, 2791.
 27. Z. Ji, G. Natu, Z. Huang and Y. Wu, *Energy & Environmental Science*, 2011, 4, 2818-2821.
 28. L. Zhu, H. B. Yang, C. Zhong and C. M. Li, *Dyes and Pigments*, 2014, 105, 97-104.
 29. M. Grätzel, *Accounts of chemical research*, 2009, 42, 1788-1798.
 30. J. Zhang, H.-B. Li, J.-Z. Zhang, Y. Wu, Y. Geng, Q. Fu and Z.-M. Su, *Journal of Materials Chemistry A*, 2013, 1, 14000-14007.
 31. H.-B. Li, J. Zhang, Y. Wu, J.-L. Jin, Y.-A. Duan, Z.-M. Su and Y. Geng, *Dyes and Pigments*, 2014, 108, 106-114.
 32. L. L. Sun, T. Zhang, J. Wang, H. Li, L. K. Yan and Z. M. Su, *RSC Advances*, 2015, 5, 39821-39827.
 33. J. Preat, C. Michaux, D. Jacquemin and E. A. Perpete, *The Journal of Physical Chemistry C*, 2009, 113, 16821-16833.
 34. M. Guo, R. He, Y. Dai, W. Shen, M. Li, C. Zhu and S. H. Lin, *The Journal of Physical Chemistry C*, 2012, 116, 9166-9179.
 35. M. Frisch, G. Trucks, H. Schlegel, G. Scuseria, M. Robb, J. Cheeseman, G. Scalmani, V. Barone, B. Mennucci and G. Petersson, *Gaussian Inc., Wallingford, CT*, 2009.
 36. T. Lu and F. Chen, *Journal of Computational Chemistry*, 2012, 33, 580-592.
 37. I. Ciofini, T. Le Bahers, C. Adamo, F. Odobel and D. Jacquemin, *The Journal of Physical Chemistry C*, 2012, 116, 11946-11955.
 38. J. Zhang, Y.-H. Kan, H.-B. Li, Y. Geng, Y. Wu and Z.-M. Su, *Dyes and Pigments*, 2012, 95, 313-321.
 39. J. Wang, H. Li, N.-N. Ma, L.-K. Yan and Z.-M. Su, *Dyes and Pigments*, 2013, 99, 440-446.
 40. J. Zhang, H.-B. Li, S.-L. Sun, Y. Geng, Y. Wu and Z.-M. Su, *Journal of Materials Chemistry*, 2012, 22, 568-576.
 41. W.-L. Ding, D.-M. Wang, Z.-Y. Geng, X.-L. Zhao and W.-B. Xu, *Dyes and Pigments*, 2013, 98, 125-135.
 42. W.-L. Ding, D.-M. Wang, Z.-Y. Geng, X.-L. Zhao and Y.-F. Yan, *The Journal of Physical Chemistry C*, 2013, 117, 17382-17398.
 43. Y. A. Duan, Y. Geng, H. B. Li, J. L. Jin, Y. Wu and Z. M. Su, *Journal of computational chemistry*, 2013, 34, 1611-1619.
 44. J. L. Jin, H. B. Li, Y. Geng, Y. Wu, Y. A. Duan and Z. M. Su, *ChemPhysChem*, 2012, 13, 3714-3722.
 45. J. Wang, M. Li, D. Qi, W. Shen, R. He and S. H. Lin, *RSC Advances*, 2014, 4, 53927-53938.
 46. B. L. Watson, B. D. Sherman, A. L. Moore, T. A. Moore and D. Gust, *Physical Chemistry*

- Chemical Physics*, 2015, 17, 15788-15796.
47. M. Guo, M. Li, Y. Dai, W. Shen, J. Peng, C. Zhu, S. H. Lin and R. He, *RSC Advances*, 2013, 3, 17515-17526.
 48. P. Gao, H. N. Tsao, C. Yi, M. Grätzel and M. K. Nazeeruddin, *Advanced Energy Materials*, 2014, 4.
 49. W. Zhu, Y. Wu, S. Wang, W. Li, X. Li, J. Chen, Z. s. Wang and H. Tian, *Advanced Functional Materials*, 2011, 21, 756-763.
 50. Y. Wu and W. Zhu, *Chemical Society Reviews*, 2013, 42, 2039-2058.

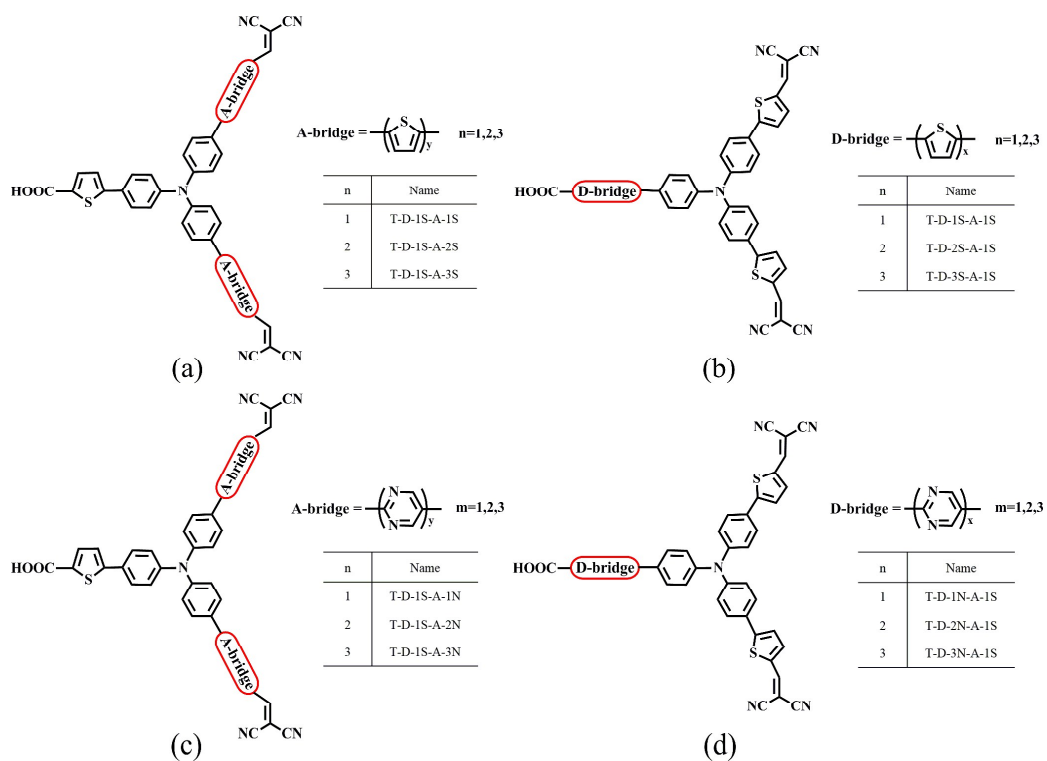


Fig. 1 Names and chemical structures of all the sensitizers.

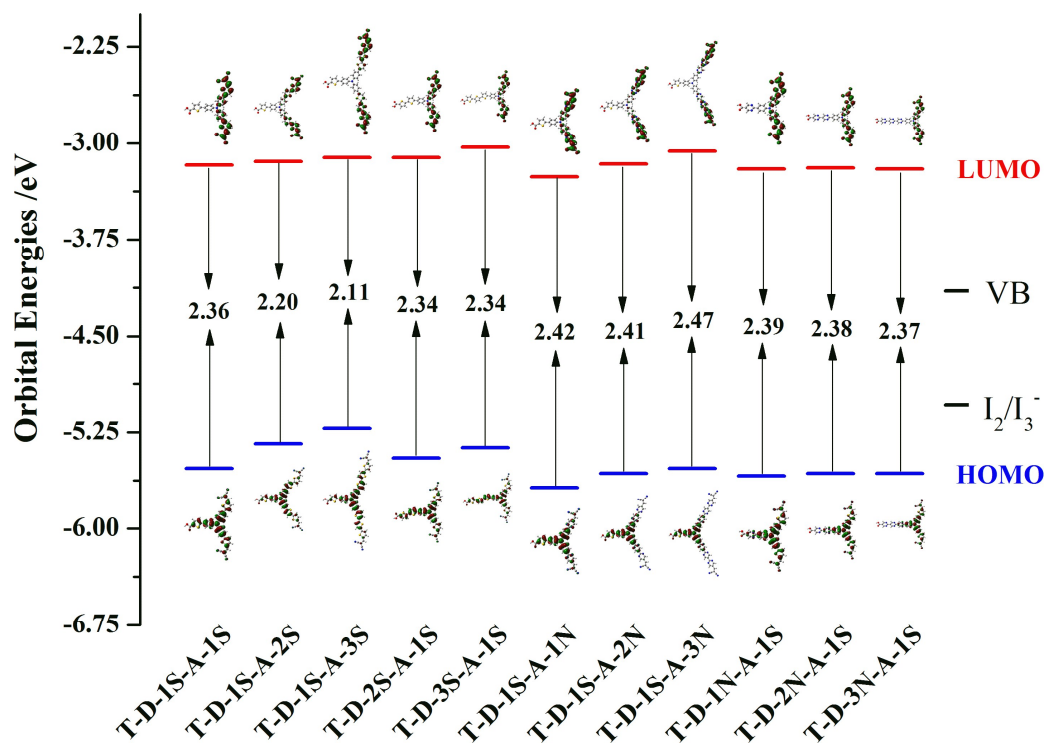


Fig. 2 Schematic energy levels of sensitizers, together with the valence band of NiO and I_2/I_3^-

redox level. All calculation is obtained at PBE0/6-31G(d) level.

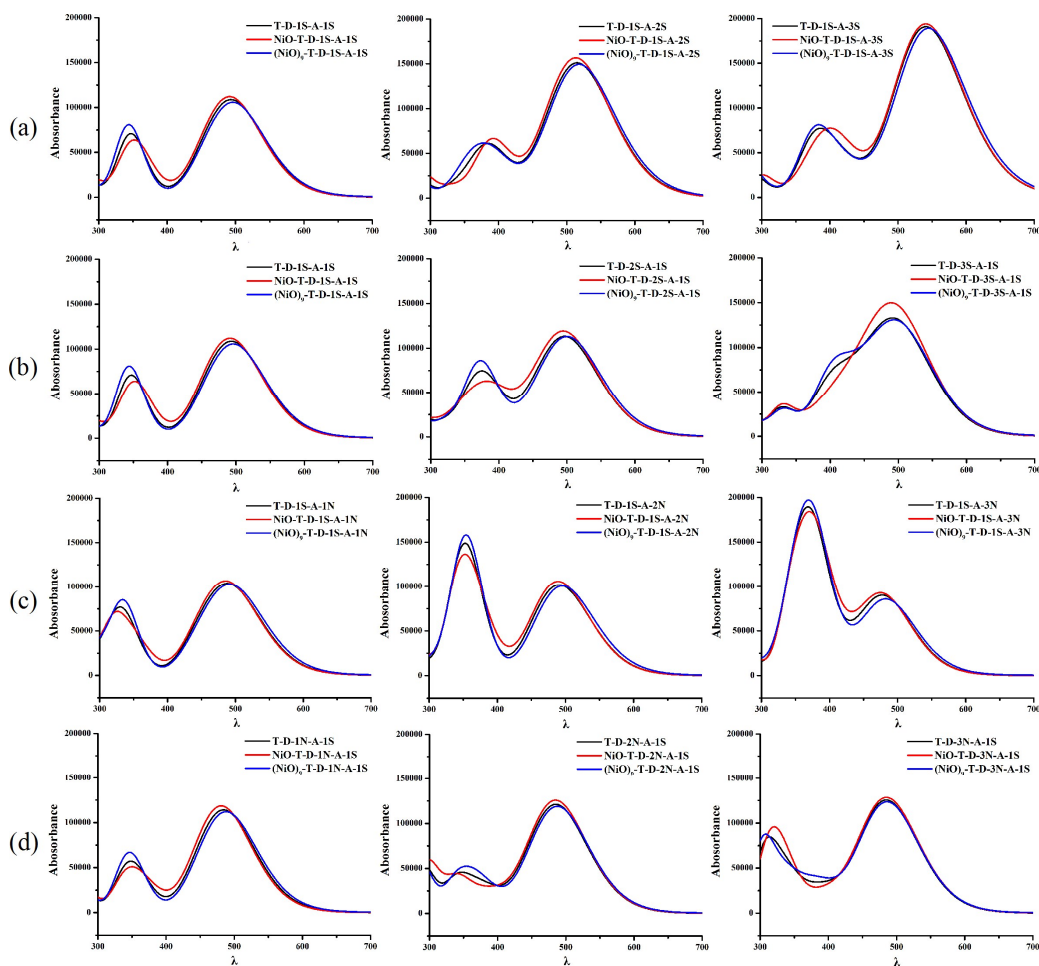


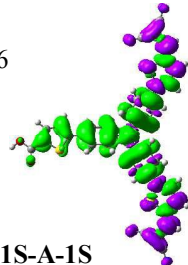
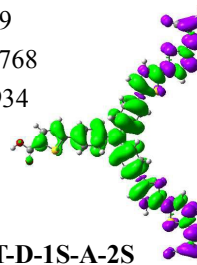
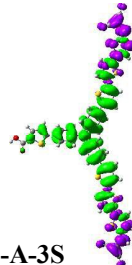
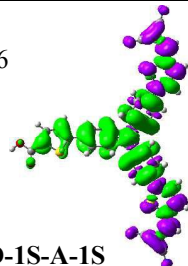
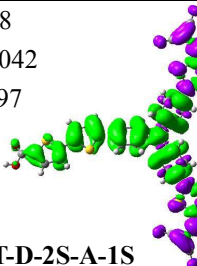
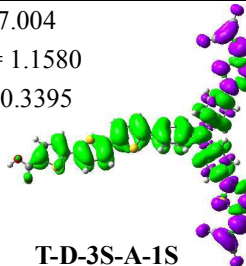
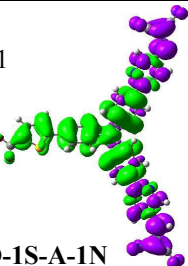
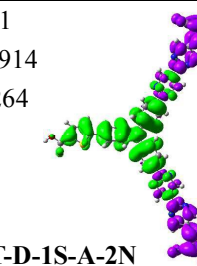
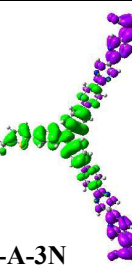
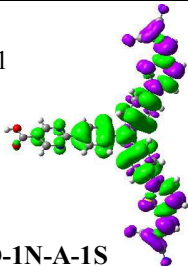
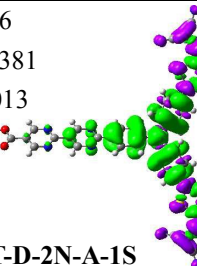
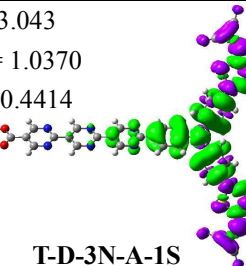
Fig. 3 Simulated absorption spectra obtained at BMK/6-31G(d) level for all the dyes, NiO-Dyes and $(\text{NiO})_9$ -Dyes in acetonitrile solution with PBE0/6-31G(d) geometries.

Table 1 Estimated maximum wavelength of spectral absorption (λ_{\max} in nm), reorganization energy ($E_{\text{reorg}}(S1)$ in eV) of the first excited state (S1), f is the oscillator strength, LHE is the light-harvesting efficiency at maximum wavelength, μ_T is the transition dipole moment from states S0 to S1. All calculation is obtained by BMK functional with 6-31G(d) basis set.

Scheme	λ_{\max} (Exp)	$E_{\text{reorg}}(S1)$	f	LHE	μ_T
T-D-1S-A-1S	498/344 (488/369)	0.13	1.85/0.73	0.9859/0.8138	30.28
T-D-1S-A-2S	527/372	0.15	1.91/0.61	0.9877/0.7545	33.03
T-D-1S-A-3S	543/387	0.18	3.30/0.84	0.9995/0.8555	58.97
T-D-2S-A-1S	504/385	0.12	1.77/0.91	0.9830/0.8770	29.34
T-D-3S-A-1S	508/415	0.10	1.71/1.01	0.9805/0.9023	28.70
T-D-1S-A-1N	497/326	0.07	1.61/0.93	0.9755/0.8825	26.41
T-D-1S-A-2N	497/351	0.08	1.48/1.62	0.9669/0.9760	24.26
T-D-1S-A-3N	482/379	0.10	1.30/1.50	0.9499/0.9684	20.70
T-D-1N-A-1S	490/341	0.14	1.86/0.70	0.9862/0.8005	29.99
T-D-2N-A-1S	493/342	0.14	1.85/0.72	0.9859/0.8095	30.03
T-D-3N-A-1S	494/313	0.14	1.85/0.83	0.9859/0.8521	30.07

Data in parentheses are experimental value.

Table 2 Electron density difference plots of electronic transition $S_0 \rightarrow S_1$ for all the dyes performed in acetonitrile solvent using BMK functional together with 6-31G(d) basis set. L is the electron transfer distance (Å), Δe is the fraction of electron exchange ($|e^-|$), Ω is overlaps between the regions of density depletion and increment (Isovalue: $4 \times 10^{-4} \text{ e au}^{-3}$).

(a)	L= 3.256 $\Delta e= 1.0506$ $\Omega= 0.3980$  T-D-1S-A-1S	L= 6.219 $\Delta e= 1.0768$ $\Omega= 0.1934$  T-D-1S-A-2S	L= 3.780 $\Delta e= 1.0838$ $\Omega= 0.3601$  T-D-1S-A-3S
(b)	L= 3.256 $\Delta e= 1.0506$ $\Omega= 0.3980$  T-D-1S-A-1S	L= 4.728 $\Delta e= 1.1042$ $\Omega= 0.6797$  T-D-2S-A-1S	L= 7.004 $\Delta e= 1.1580$ $\Omega= 0.3395$  T-D-3S-A-1S
(c)	L= 4.515 $\Delta e= 1.1681$ $\Omega= 0.2726$  T-D-1S-A-1N	L= 6.261 $\Delta e= 1.2914$ $\Omega= 0.1264$  T-D-1S-A-2N	L= 8.023 $\Delta e= 1.3276$ $\Omega= 0.0522$  T-D-1S-A-3N
(d)	L= 2.985 $\Delta e= 1.0391$ $\Omega= 0.3988$  T-D-1N-A-1S	L= 3.076 $\Delta e= 1.0381$ $\Omega= 0.4013$  T-D-2N-A-1S	L= 3.043 $\Delta e= 1.0370$ $\Omega= 0.4414$  T-D-3N-A-1S

Electron densities move from the green area to the purple area.

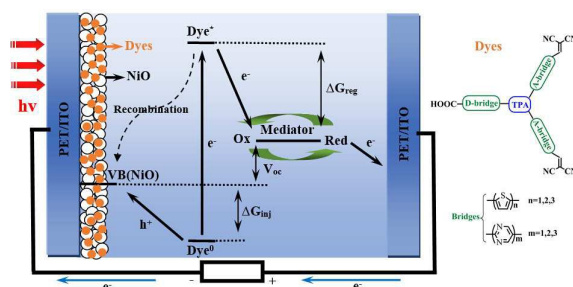
Table 3 Computed 0-0 transition energy (E_{0-0} in eV), oxidized potential ($E_{\text{OX(dye)}}$ in eV) and reduced potential ($E_{\text{red(dye)}}$ in eV) of dyes in the ground state, ΔG_{inj} , ΔG_{reg} and ΔG_{CR} are the driving force of hole injection, regeneration and recombination (eV) respectively, All calculation is obtained by PBE0 functional with 6-31G(d) basis set.

Scheme	E_{0-0}	$E_{\text{ox(dye)}}$	$E_{\text{red(dye)}}$	ΔG_{inj}	ΔG_{reg}	ΔG_{CR}
T-D-1S-A-1S	2.36	5.21	3.22	-0.54	-0.93	1.82
T-D-1S-A-2S	2.20	5.04	3.29	-0.45	-0.86	1.75
T-D-1S-A-3S	2.11	4.91	3.33	-0.40	-0.82	1.71
T-D-2S-A-1S	2.34	5.10	3.21	-0.51	-0.94	1.83
T-D-3S-A-1S	2.34	5.03	3.21	-0.51	-0.94	1.83
T-D-1S-A-1N	2.42	5.28	3.38	-0.76	-0.77	1.66
T-D-1S-A-2N	2.41	5.24	3.51	-0.88	-0.64	1.53
T-D-1S-A-3N	2.47	5.20	3.55	-0.98	-0.60	1.49
T-D-1N-A-1S	2.39	5.28	3.28	-0.63	-0.87	1.76
T-D-2N-A-1S	2.38	5.26	3.22	-0.56	-0.93	1.82
T-D-3N-A-1S	2.37	5.26	3.26	-0.59	-0.89	1.78

Effect of “push-pull” sensitizers with modified conjugation bridges on the performance of p-type dye-sensitized solar cells

Fengying Zhang, Pei Yu, Wei Shen, Ming Li, Rongxing He*

Graphical abstract:



P-type “push-pull” sensitizers with modified conjugation bridges (thiophene units and pyrimidine units) are investigated theoretically.

* To whom correspondence should be addressed. E-mail: herx@swu.edu.cn.